Inorg. Chem. **2005**, *44*, 8145–8155

Coordination Chemistry of a New Rigid, Hexadentate Bispidine-Based Bis(amine)tetrakis(pyridine) Ligand

Christian Bleiholder,[†] Heidi Börzel,[†] Peter Comba,*[,†] Rosana Ferrari,[†] Matthias Heydt,[†] Marion Kerscher,[†] Shigemasa Kuwata,[†] Gabor Laurenczy,[‡] Geoffrey A. Lawrance,[§] Achim Lienke,[†] Bodo Martin,[†] Michael Merz,[†] Bernd Nuber,[†] and Hans Pritzkow[†]

Universität Heidelberg, Anorganisch-Chemisches Institut, Im Neuenheimer Feld 270, D-69120 Heidelberg, Germany, Ecole Polytechnique Fédérale de Lausanne, Institut des Sciences et Ingénieric Chimiques (ISIC) BCH LCCO, CH-1015 Lausanne, Switzerland, and Chemistry, School of Environment and Life Sciences, University of Newcastle, Callaghan, NSW 2308, Australia

Received August 5, 2005

The hexadentate bispidine-based ligand 2,4-bis(2-pyridyl)-3,7-bis(2-methylenepyridine)-3,7-diazabicyclo[3.3.1]nonane-9-on-1,5-bis(carbonic acid methyl ester), L^{6m}, with four pyridine and two tertiary amine donors, based on a very rigid diazaadamantane-derived backbone, is coordinated to a range of metal ions. On the basis of experimental and computed structural data, the ligand is predicted to form very stable complexes. Force field calculations indicate that short metal–donor distances lead to a buildup of strain in the ligand; that is, the coordination of large metal ions is preferred. This is confirmed by experimentally determined stability constants, which indicate that, in general, stabilities comparable to those with macrocyclic ligands are obtained with the relative order $Cu^{2+} > Zn^{2+} \gg Ni^{2+} < Co^{2+}$, which is not the typical Irving–Williams behavior. The preference for large M–N distances also emerges from relatively high redox potentials (the higher oxidation states, that is, the smaller metal ions, are destabilized) and from relatively weak ligand fields (dd-transition, high-spin electronic ground states). The potentiometric titrations confirm the efficient encapsulation of the metal ions since only 1:1 complexes are observed, and, over a large pH range, ML is generally the only species present in solution.

Introduction

The fit or misfit of a specific metal ion to a given ligand is of importance for the stabilization or the activation of the corresponding metal complex. This is a fundamental feature in areas where the aims are metal ion selectivity (selective stabilization) or the specific activation of substrates (destabilization, energization).[1−5] Basic requirements for ligands with this feature are high degrees of preorganization and complementarity[6−8] with respect to a specific metal ion and coordination geometry. Both efficient preorganization and high complementarity require rigidity; a high degree of flexibility (conformational freedom) and elasticity (ease of distortion of a specific conformer) lead to a decreasing ability of the ligand to enforce a specific geometry and, therefore, lead to decreasing selectivity, both with respect to thermodynamics and reactivity. A high degree of complementarity also requires a good fit between the electronic preferences of the metal ion and the donors; this is included in the "generalized double complementarity concept" but is often neglected.[1,9] In addition to ligand elasticity, the elasticity of the coordination sphere needs also to be considered; that is, a very rigid ligand (such as 1,10-phenanthroline or the

* Author to whom correspondence should be addressed. Fax: +49−6221−54 6617, e-mail: peter.comba@aci.uni-heidelberg.de.
† Universität Heidelberg.
‡ Ecole Polytechnique Fédérale de Lausanne.
§ University of Newcastle.

(1) Comba, P.; Schiek, W. *Coord. Chem. Rev.* **2003**, *238−239*, 21.
(2) Hancock, R. D.; Martell, A. E. *Chem. Rev.* **1989**, *89*, 1975.
(3) Comba, P. *Coord. Chem. Rev.* **1999**, *185*, 81.
(4) Comba, P. *Coord. Chem. Rev.* **2000**, *200−202*, 217.
(5) Frausto da Silva, J. J. R.; Williams, R. J. P. *The Biological Chemistry of the Elements*; Clarendon Press: Oxford, U. K., 1999.
(6) Cram, D. J.; Lein, G. M.; Kaneda, T.; Helgeson, R. C.; Knobler, C. B.; Maverick, E.; Trueblood, K. N. *J. Am. Chem. Soc.* **1981**, *103*, 6228.
(7) Artz, S. P.; Cram, D. J. *J. Am. Chem. Soc.* **1984**, *106*, 2160.
(8) Cram, D. J.; Kaneda, T.; Helgeson, R. C.; Brown, S. B.; Knobler, C. B.; Maverick, E.; Trueblood, K. N. *J. Am. Chem. Soc.* **1985**, *207*, 3645.
(9) Lindoy, L. F. *The Chemistry of Macrocyclic Ligand Complexes*; Cambridge University Press: Cambridge, New York, 1989.

10.1021/ic0513383 CCC: $30.25
Published on Web 09/23/2005

Chart 1

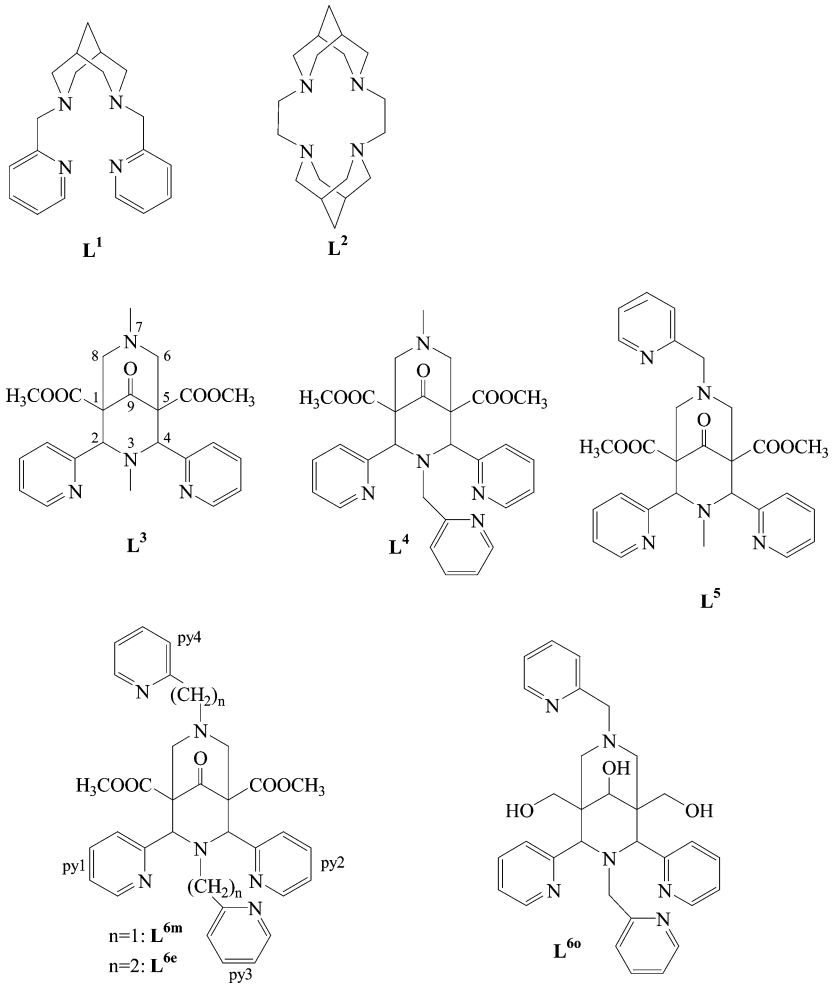

bispidine ligands discussed here) might tolerate large variations in metal−donor distances, and this also leads to a reduction of the metal ion selectivity.[1] Furthermore, in the original definition of ligand preorganization, solvation of the donor groups is also included.[6−8] Macrocyclic ligands are often used when rigidity, preorganization, and complementarity are of importance,[9,10] but rigid acyclic ligands have also been shown to be able to enforce a specific shape of the chromophore.[11,12] Reinforcement of the ligand backbone has been shown to be an important tool for enhancing the rigidity and selectivity.[13−16]

Ligands with bispidine elements (bispidine = 3,7-diazabicyclo[3.3.1]nonane) in the backbone are known to be very rigid;[1,11,12,17−21] examples of various bispidine-type ligands are given in Chart 1 (for the numbering scheme, see L^3 and L^6 in Chart 1; note that the IUPAC numbering, used throughout in the discussion, and the crystallographic numbering schemes, see below, are different). L^1 enforces a distorted square planar geometry.[11,12] L^2 is an extremely rigid cyclam-type macrocycle which enforces square planar geometry and an extremely strong ligand field with copper(II).[17] L^{3-6} enforce square pyramidal (L^3, with one coligand, strong in-plane bonding, N7 usually is the axial donor) or octahedral coordination geometry (L^3 with 2 coligands in cis orientation, $L^{4,5}$ with 1 coligand);[1,22−25] seven-coordinate complexes with L^{3-5} have also been observed. [19,26] Coordinating substituents other than pyridine in the 2, 3, 4, and 7 positions (for numbering, see L^3 in Chart 1) have been

(10) Dietrich, B.; Viout, P.; Lehn, J.-M. *Macrocyclic Chemistry. Aspects of Organic, Inorganic and Supramolecular Chemistry*; VCH: New York, 1993.
(11) Hosken, G. D.; Hancock, R. D. *J. Chem. Soc., Chem. Commun.* **1994**, 1363.
(12) Hosken, G. D.; Allan, C. C.; Boeyens, J. C. A.; Hancock, R. D. *J. Chem. Soc., Dalton Trans.* **1995**, 3705.
(13) Schwarzenbach, G.; Gut, R.; Anderegg, G. *Helv. Chim. Acta* **1954**, *37*, 937.
(14) Wainright, K. P.; Ramasubby, A. *J. Chem. Soc., Chem. Commun.* **1982**, 277.
(15) Wainright, K. P. *Inorg. Chem.* **1980**, *19*, 1396.
(16) Hancock, R. D. *Pure Appl. Chem.* **1993**, *65*, 941.
(17) Comba, P.; Pritzkow, H.; Schiek, W. *Angew. Chem.* **2001**, *113*, 2556.
(18) Comba, P.; Lienke, A. *Inorg. Chem.* **2001**, *40*, 5206.
(19) Comba, P.; Kerscher, M.; Merz, M.; Müller, V.; Pritzkow, H.; Remenyi, R.; Schiek, W.; Xiong, Y. *Chem. Eur. J.* **2002**, *8*, 5750.
(20) Comba, P.; Kerscher, M.; Roodt, A. *Eur. J. Inorg. Chem.* **2004**, 4640.
(21) Comba, P.; Kerscher, M. *Cryst. Eng.* **2004**, *6*, 197.
(22) Börzel, H.; Comba, P.; Katsichtis, C.; Kiefer, W.; Lienke, A.; Nagel, V.; Pritzkow, H. *Chem. Eur. J.* **1999**, *5*, 1716.
(23) Börzel, H.; Comba, P.; Hagen, K. S.; Kerscher, M.; Pritzkow, H.; Schatz, M.; Schindler, S.; Walter, O. *Inorg. Chem.* **2002**, *41*, 5440.
(24) Börzel, H.; Comba, P.; Hagen, K. S.; Merz, M.; Lampeka, Y. D.; Lienke, A.; Linti, G.; Pritzkow, H.; Tsymbal, L. V. *Inorg. Chim. Acta* **2002**, *337*, 407.
(25) Comba, P.; Merz, M.; Pritzkow, H. *Eur. J. Inorg. Chem.* **2003**, 1711.
(26) Bukowski, M. R.; Comba, P.; Limberg, C.; Merz, M.; Que, L., Jr.; Wistuba, T. *Angew. Chem.* **2004**, *116*, 1303.

reported,[24,25,27] and oligo-nucleating ligands, bridged through N7, have been described.[22−24,28]

A common and central feature of L^{1-6} is the extremely rigid and highly preorganized 3,7-diazaadamantane-derived, reinforced six-membered chelate ring of the bidentate, unsubstituted bispidine fragment. Chair-boat conformations are only rarely observed in metal-free bispidine compounds.[1,29,30] The approximately constant N3···N7 distance (about 2.9 Å, see discussion of the structures below) is a good measure for the rigidity of the bispidine fragment. Tetradentate bispidine ligands with pyridine (and other) donor groups in the 2 and 4 positions (L^3) have "alternative complementarities" with respect to the metal−N3/metal−N7 bond distances.[1,18,19,21] This leads to interesting distortions of the chromophores, in particular, for the Jahn−Teller active copper(II) ion.[21,27,28,31] Also of specific interest is the strong bonding and activation of in-plane coligands.[18,21,26] Additional pyridine donors at N3 or N7 (pentadentate ligands $L^{4,5}$) lead to a marked variation in these structural and emerging thermodynamic effects and reactivities,[21,24−26] and it was of interest to probe the consequences due to hexacoordination in $L^{6m,e,o}$.

While the unsubstituted bidentate bispidine fragment is very rigid, its complex with a metal ion is not; that is, apart from the generally weak $C_{backbone}$−N−metal angular potential, there is little constraint for the distance of the metal ion from the N3···N7 vector; that is, the unsubstituted bispidine ligand tolerates large differences in metal−donor distances (elasticity of the coordination sphere) and is not very size-selective.[1] Structural studies of complexes with the tetradentate ligand L^3 indicate that the two extra donors in the 2 and 4 positions do not dramatically alter this situation;[19] the computation of hole-size curves with force field methods[32] supports this interpretation.[1,19]

Here, we report the syntheses and coordination chemistry of the bispidine ligands L^{6m}, L^{6e}, and L^{6o} with cobalt(II), nickel(II), copper(II), zinc(II), and lithium(I), including structural data, stability constants, spectroscopy, and electrochemistry. L^{6m} is a derivative of both tetradentate ligands, L^1 (square planar or trans-octahedral coordination geometry) and L^3 (cis-octahedral coordination geometry). L^1 was reported[11,12] to be rigid and inelastic; the computed "hole-size curves" were steep (note that these were computed with another technique than what we used), suggesting a high metal ion selectivity; there was no comment on the elasticity of the coordination sphere, but the reports suggest that it is inelastic. L^3, on the other hand, is also rigid, but the coordination sphere is elastic; hence, the potential energy surface is flat and the ligand, on the basis of steric effects alone, is unselective, except for the destabilization of relatively small metal ions (M−L < 2.0 Å, vide infra). Interestingly, the conclusions drawn from an analysis of observed stability constants and the computation of the hole size state that the bispidine cap in L^1 enforces small metal−$N_{bispidine}$ distances.[12] It, therefore, was of particular interest to study this specific aspect with our hexadentate ligands $L^{6m,e,o}$.

Results and Discussions

Syntheses. The ligands $L^{6m,e}$ were prepared in good yield in analogy to the long-known bispidine L^3,[33,34] by two consecutive Mannich condensations, outlined in detail in the Experimental Section.[24] Recrystallization of the ligands in ethanol (or methanol) is a key step in the synthesis of bispidine ligands in general. It not only purifies but also isomerizes the crude products to the required endo−endo configuration [2(R),4(S) or vice versa]. Kinetically, the formation of the exo−endo isomer is favored, and this has one of the two pyridine donors at C2 or C4 in a position which points out of the coordination pocket (characterization of the isomers by ^{1}H NMR spectroscopy, for details regarding the characterization and isomerization, see ref 35). With respect to the stability of the metal-free ligands, acid-catalyzed retro-Mannich reactions (even at relatively high pH) are the most severe problem, and in basic solution (pH > 10), there is slow decomposition of the ligand. Therefore, for a number of applications, the ligands were reduced to the corresponding triols, following a protocol developed for L^3 (detailed in the Experimental Section).[36] Metal complexes were obtained from ethanolic solutions of equimolar amounts of the ligands and metal salts.

Structural Properties. Data from X-ray crystal structural analyses of the metal-free ligand L^{6m} are presented in Figure 1 and Table 1; ORTEP plots[37] of the complex cations $[Ni(L^{6m})]^{2+}$, $[Cu(L^{6m})]^{2+}$, $[Zn(L^{6m})]^{2+}$, $[Li(L^{6o})]^{2+}$, $[Co(L^{6e})]^{2+}$, and $[Cu(L^{6e})]^{2+}$ are shown in Figure 2; the corresponding data are also listed in Table 1 (note that the crystallographic numbering scheme, see Figure 2, is different from the IUPAC numbering, given in Chart 1 and used throughout the discussion; both are given in Table 1). The structural properties of L^{6m} and its complexes (and those of $L^{1,3-5}$) have also been analyzed by force field calculations, and these results are given in Table 2.

As for other metal-free bispidine ligands,[1,19,21,22,38] the bispidine backbone in L^{6m} is highly preorganized[1] with a N3···N7 distance only slightly larger than that in most complexes (lone-pair repulsion). The pyridine donors at C2 and C4 (py1 and py2) are rotated away in the metal-free

(27) Comba, P.; Lopez de Laorden, C.; Pritzkow, H. *Helv. Chim. Acta* **2005**, *88*, 647.
(28) Comba, P.; Hauser, A.; Kerscher, M.; Pritzkow, H. *Angew. Chem.* **2003**, *115*, 4675.
(29) Quast, W.; Müller, B. *Chem. Ber.* **1980**, *113*, 2959.
(30) Siener, T.; Holzgrabe, U.; Drosihn, S.; Brandt, W. *J. Chem. Soc., Perkin Trans. 2* **1999**, 1827.
(31) Comba, P.; Martin, B.; Prikhod'ko, A.; Pritzkow, H.; Rohwer, H. *Compt. Rendus Chim.* In press.
(32) Comba, P.; Okon, N.; Remenyi, R. *J. Comput. Chem.* **1999**, *20*, 781.
(33) Samhammer, A.; Holzgrabe, U.; Haller, R. *Arch. Pharm. (Weinheim, Ger.)* **1989**, *322*, 551.
(34) Holzgrabe, U.; Ericyas, E. *Arch. Pharm. (Weinheim, Ger.)* **1992**, *325*, 657.
(35) Siemer, T.; Holzgrabe, U.; Drosihn, S.; Brandt, W. *J. Chem. Soc., Perkin Trans. 2* **1999**, 1827.
(36) Comba, P.; Kanellakopulos, B.; Katsichtis, C.; Lienke, A.; Pritzkow, H.; Rominger, F. *J. Chem. Soc., Dalton* Trans. **1998**, 3997.
(37) Johnson, C. K. *ORTEP, A Thermal Ellipsoid Plotting Program*; Oak National Laboratories: Oak Ridge, TN, 1965.
(38) Börzel, H.; Comba, P.; Hagen, K. S.; Katsichtis, C.; Pritzkow, H. *Chem. Eur. J.* **2000**, *6*, 914.

Table 1. Selected Experimental Structural Data of L^{6m}, $[Li(L^{6o})]^+$, $[Ni(L^{6m})]^{2+}$, $[Cu(L^{6m})]^{2+}$, $[Zn(L^{6m})]^{2+}$, $[Co(L^{6e})]^{2+}$, and $[Cu(L^{6e})]^{2+}$ (Distances in Å, Angles in Degrees; the Ligands in the Complexes of L^{6m} and L^{6e} are Hydrated, See Text)

	L^{6m}	$[Li(L^{6o})]^{2+}$	$[Ni(L^{6m})]^{2+}$	$[Cu(L^{6m})]^{2+}$		$[Zn(L^{6m})]^{2+}$	$[Co(L^{6e})]^{2+}$		$[Cu(L^{6e})]^{2+}$
				Distances					
M−N3; N1		2.120(6)	2.074(3)	2.087(3)	2.093(3)	2.166(2)	2.138(5)	2.110(4)	2.016(2)
M−N7; N2		2.236(6)	2.156(3)	2.045(3)	2.037(3)	2.234(2)	2.224(5)	2.253(5)	2.195(2)
$M-N_{py1}$; N3		2.272(6)	2.101(3)	2.280(3)	2.261(3)	2.170(2)	2.172(5)	2.126(5)	2.006(2)
$M-N_{py2}$; N4		2.315(6)	2.153(3)	2.573(3)	2.608(3)	2.285(3)	2.147(5)	2.157(5)	2.024(2)
$M-N_{py3}$; N5		2.191(6)	2.081(3)	2.009(3)	2.012(3)	2.112(3)	2.223(5)	2.251(5)	
$M-N_{py4}$; N6		2.092(6)	2.078(3)	2.028(3)	2.031(3)	2.069(2)	2.132(5)	2.132(5)	1.966(2)
$\sum_{i=1}^{6}(M-N_i)$		13.23	12.64	13.02	13.04	13.04	13.01	13.07	
N3···N7; N1, N2	2.94	2.89	2.88	2.83	2.84	2.90	2.91	2.88	2.90
$N_{py1}\cdots N_{py2}$; N3, N4	4.59[a]	4.47	4.18	4.67	4.70	4.34	4.25	4.21	3.96
$N_{py3}\cdots N_{py4}$; N5, N6	8.49	3.56	3.35	3.19	3.22	3.48	3.15	3.17	
H6···H6′		2.48	2.20	2.24	2.26	2.41	2.37	2.47	
				Angles					
N3−M−N7; N1, N2		83.0 (2)	85.81(11)	86.43(12)	86.90(12)	82.59(8)	83.7(2)	82.54(17)	87.03(8)
$N3-M-N_{py4}$; N1, N6		159.8(3)	163.34(12)	154.39(13)	153.31(13)	157.11(9)	175.6(2)	174.48(19)	171.34(9)
$N7-M-N_{py3}$; N2, N5		164.6(3)	169.23(11)	172.12(12)	171.36(13)	165.55(8)	172.3(2)	173.36(18)	-
$N_{py1}-M-N_{py2}$; N3, N4		154.3(3)	158.97(11)	148.53	149.21	153.35(8)	158.8(2)	158.84(18)	158.31(9)
				Torsions					
$N3-C2-C_A-N_{py1}$; N1, N3	−33.89[a]	−44.06	−40.02	−41.86	−43.47	−41.46	−36.98	−44.10	−34.98
$N3-C4-C_{A'}-N_{py2}$; N1, N4	39.41[a]	43.55	39.93	42.93	46.21	39.30	45.82	35.82	33.71
				Twist Angles between Pyridine Rings					
py1···py2	31.10	36.87	34.97	41.34	39.95	36.61	32.10	31.87	23.89
py3···py4	65.24	36.79	34.46	38.48	37.43	35.52	37.49	36.38	

[a] N3−C2−C1−Npy1 adjusted by 180°.

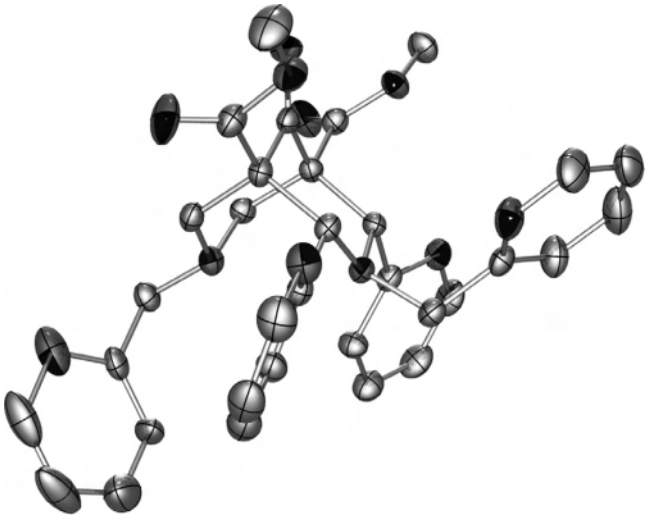

Figure 1. ORTEP[37] plot of the bispidine L^{6m}.

ligands from the coordination site by approximately 180°, and the two other pyridine donors at N3 and N7 (py3 and py4) are also in a geometry different from that in the complexes. That is, with respect to the pyridine donors, the ligands are not preorganized, but conformational reorganization is expected to be a low-energy process, and the conformation in the complex is, if at all, not significantly less stable; the major effect is lone-pair repulsion, which disappears upon coordination to a metal ion. The structures of the metal complexes (see Figure 2) are all quite similar; significant differences are only observed in the structures of the Jahn−Teller labile copper(II) compounds. All keto groups at C9 are hydrated [except in the lithium(I) complex, where the reduced triol ligand L^{6o} was used], as generally observed with bispidines if the complexation reactions are not performed under strictly water-free conditions (for simplicity, this is not included in the nomenclature used here).[1,19,28,39] This hydration may be responsible for the release of an extra proton, when the complexes are titrated in the basic pH region, yielding a relatively constant pK_a value of 9 (see below and Table 3).

As in the copper(II) complex of L^1,[12] the planarity of the $M-N3-N7-N_{py3}-N_{py4}$ fragment is distorted as a result of repulsion of the ortho protons of these two pyridine rings (py3 and py4). The corresponding H6···H6′ distances in all experimental structures (see Table 1) are 2.2−2.5 Å. For L^{6m}, this distortion primarily involves the pyridine ring py4, substituted at N7 (see Figure 2). The resulting asymmetry is responsible for a significant difference in the bonding to the remaining two pyridine groups (py1 and py2). As expected, this is not observed in complexes of L^{6e}, where both six-membered chelate rings, involving py3 and py4, are puckered.

In complexes of the tetradentate ligand L^3, two clusters of structures with different positions of the metal ion in the ligand cavity have been observed, one with M−N3 < M−N7, the other with M−N3 ≥ M−N7;[19] in particular for the copper(II) complexes of L^3, there is a large difference between the two bond distances to the amine donors, due to the Jahn−Teller lability, with Cu−N3 approximately 2.03 Å and Cu−N7 approximately 2.28 Å.[1,18,19] Observations with the copper(II) complex of L^4 indicate that there are two isomers with elongation along either the N7···py3 or the py1···py2 axis.[28] With derivatives of L^3 with α-methylated pyridine or quinoline groups, "Jahn−Teller isomers" with elongation along all three possible axes have been observed, dependent on the coligands (Cl^-, OH_2, $NCCH_3$, or ONO_2^-).[21,25,27,31,38] Therefore, it is not surprising that the copper(II) complex of L^{6m} has an elongation along the py1···py2 axis (note the asymmetry in the bonding to these two pyridine groups, which indicates that the structure is between six- and five-coordinate; see also the discussion of

(39) Comba, P.; Nuber, B.; Ramlow, A. *J. Chem. Soc., Dalton Trans.* **1997**, 347.

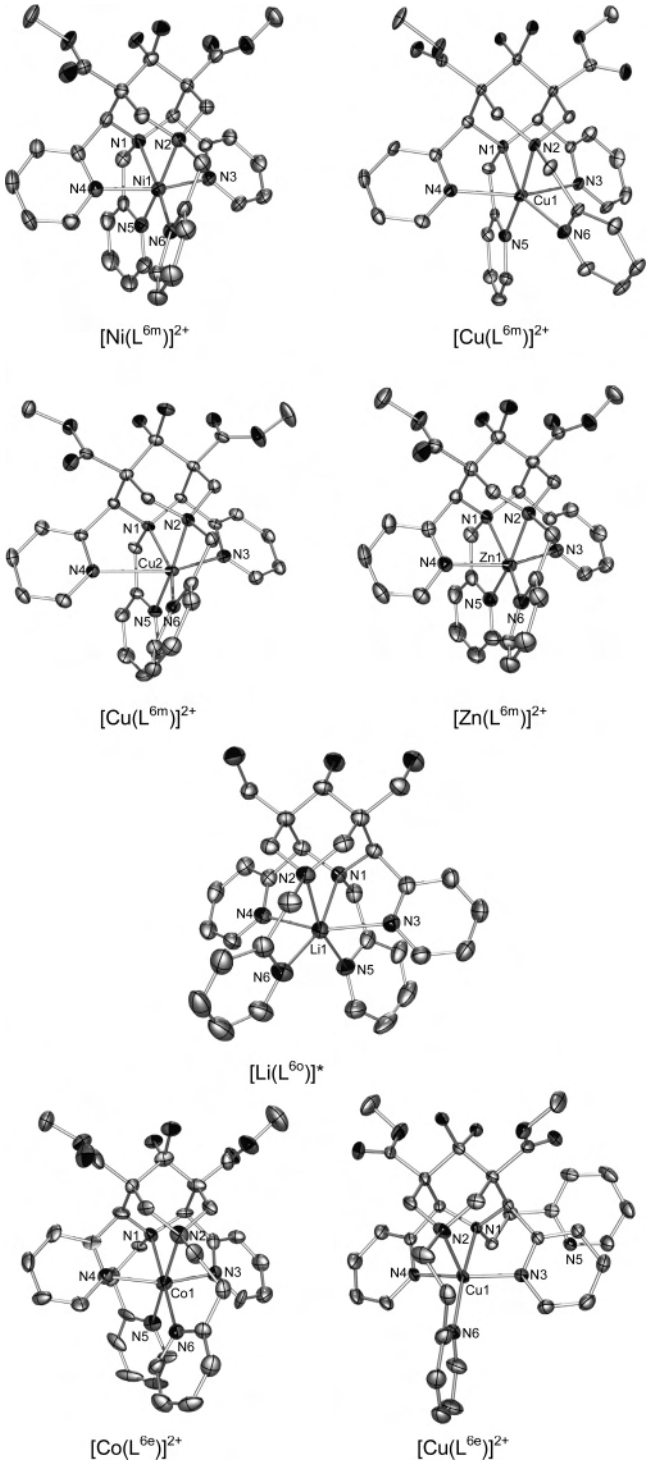

Figure 2. ORTEP[37] plots of the molecular cations of $[Ni(L^{6m})](ClO_4)_2 \cdot 3H_2O$, $[Cu(L^{6m})](ClO_4)_2 \cdot 2H_2O$ (two independent molecular cations), $[Zn(L^{6m})](ClO_4)_2 \cdot 3H_2O$, $[Li(L^{6o})]ClO_4 \cdot 0.5CH_3OH$, $[Co(L^{6e})](PF_6)_2 \cdot H_2O$, and $[Cu(L^{6e})](ClO_4)_2 \cdot H_2O$.

the force field calculations, below). Interestingly, the copper(II) complex with L^{6e} is genuinely five-coordinate with an elongated Cu−N7 bond. This probably is due to the more flexible bonds to py3 and py4 and the less-favored six-membered chelate rings involving these donors, an effect which also emerges from the structural data of the corresponding cobalt(II) complex (see Table 1). Further indications for the flat potential energy surfaces of bispidine complexes with multiple shallow minima[21] are the structure of the zinc(II) complex of L^{6m}, which has Zn−N7 > Zn−N3, while complexes with L^3 have Zn−N3 > Zn−N7[19], and that for copper(II) with L^{6m}, where Cu−N3 > Cu−N7, while with L^3, Cu−N3 ≪ Cu−N7 (see Table 1).

In contrast to expectations based on published data and associated interpretations of the tetradentate ligand L^1,[11,12] but as expected from experiments and computations with L^3, the two hexadentate ligands tolerate rather large variations in metal ion size: 12.6 Å < $\sum_{i=1}^{6}(M - N_i)$ < 13.2 Å (see Table 1). The individual bond distances are in the expected ranges for the corresponding metal ions,[40] generally at the longer limit of the corresponding average distances; for example, they are approximately 0.01 Å longer than distances to the hexadentate tpen ligand [tpen = N,N,N′,N′-tetra(2′-pyridylmethyl)ethane-1,2-diamine],[41,42] and this is confirmed by force field calculations, which indicate that the ligand does not induce severe strain on the metal ions nor vice versa (see Table 2; see also the ligand field and redox properties). Admittedly, some of the computed bond distances are only in fair agreement with the observed structural data. However, the sums over all six M−N distances each [$\sum_{i=1}^{6}(M - N_i)$] are in very good agreement (see Tables 1 and 2). The discrepancies in individual bond distances are a result of the flat potential energy surface and the resulting high elasticity of the coordination geometries. Studies based on experimental and computed structures, primarily with L^3 [19] but also with L^4,[21,28] L^5, and L^6,[43] indicate that the metal center can adopt various positions within the ligand cavity and enforce various types of distortions to the ligand (primarily on the basis of variations of the torsional angles involving the pyridine donors, and these have low energy barriers). In the present study, we did not evaluate the conformational space (this also applies for the hole-size curves discussed below), and the two relevant structural parameters, therefore, are $\sum_{i=1}^{6}(M - N_i)$ and N3···N7, where excellent agreement is observed between computed and experimental data sets (see Tables 1 and 2).

The fact that coordination of various metal ions to the bispidine ligands does not induce much strain (specifically for M−N > 2.1Å) is also confirmed by the cavity size calculations,[32] which were performed both with and without inclusion of specific metal−donor stretching and donor−metal−donor angle bending terms. The metal-ion-independent computations for the ligands L^1, L^3, L^4, L^5, and L^{6m} are presented in Figure 3. Here, no metal-based stretching or bending potentials are included. The only restrictive force for a variation of the six individual metal−donor bonds (that is, the displacement of the metal ion within or out of the rigid cavity) is an angular distortion of the metal−donor−backbone terms (directionality of the donor lone pairs), but

(40) Orpen, A. G.; Bramner, L.; Allen, F. H.; Kennard, O.; Watson, D. G.; Taylor, R. *J. Chem. Soc., Dalton Trans.* **1989**, 1.
(41) Eriksen, J.; Goodson, P.; Hazell, A.; Hodgson, P. D.; Michelsen, K.; Monsted, O.; Rasmussen, J. C.; Toftlund, H. *Acta Chem. Scand.* **1999**, *53*, 1083.
(42) daLuz, D.; Franco, C. V.; Vancato, I.; Neves, A.; Primerano Mascarenhas, Y. *J. Coord. Chem.* **1992**, *26*, 269.
(43) Bleiholder, C.; Comba, P.; Heydt, M. Unpublished results.

Table 2. Selected Computed Structural Parameters and Strain Energies of Transition Metal Complexes with L^{6m} and Analogues

	$Cr^{3+}(L^{6m})$	$Co^{3+}(L^{6m})$	$Co^{2+}(L^{6m})$	$Ni^{2+}(L^{6m})$	$Cu^{2+}(L^{6m})^a$	$Cu^{2+}(L^{6m})^b$	$Zn^{2+}(L^{6m})$	$Ni^{2+}(L^3)$	$Ni^{2+}(L^1)$
					Distances				
M−N3	2.11	1.96	2.18	2.15	1.99	2.06	2.25	2.17	2.18
M−N7	2.11	2.02	2.15	2.13	2.48	2.01	2.2	2.1	2.18
$M-N_{py1}$	2.04	1.94	2.13	2.09	2.06	2.56	2.18	2.77	2.23
$M-N_{py2}$	2.03	1.92	2.12	2.07	1.99	2.45	2.18	2.61	2.23
$M-N_{py3}$	2.06	1.94	2.14	2.11	2.26	1.98	2.18		
$M-N_{py4}$	2.03	1.93	2.11	2.07	2.02	2.03	2.12		
$\sum_{i=0}^{6}(M-N)_i$	12.38	11.71	12.83	12.62	12.8	13.09	13.11	9.65	8.82
N3···N7	2.96	2.76	3.06	3.02	2.96	2.91	3.11	3.02	2.96
$N_{py1}\cdots N_{py2}$	3.99	3.82	4.13	4.06	3.99	4.82	4.21	5.11	3.71
					Angles				
N3−M−N7	89.3	87.8	89.7	89.9	82.3	91.3	88.8	90	
$N3-M-N_{py4}$	168.8	170.5	167.4	168.4	155.3	154	165.9		
$N7-M-N_{py3}$	166.3	166.2	166.9	166.9	166.4	170.3	165.5		
$N_{py3}-M-N_{py2}$	157.5	164.2	153.3	155.4	160.7	1407.5	150.6	143.92	112.33
					Torsions				
$N3-C2-CA-N_{Py1}$	38.3	31.7	41.38	40.21	21.9	42.52	42.99	46.48	
$N3-C4-CA-N_{Py2}$	38.13	28.1	41.33	40.45	21.71	43.14	43.29	10.63	
					Twist Angles				
N(3)/N(4):Py1/Py2	29.32	13.64	35.36	33.57	10.19	38.33	37.14	37.91	
N(5)/N(6):Py3/Py4	22.9	26.84	18.48	20.73	28.46	45.9	17.36		
					Energies				
E_{strain}	145.6	196.2	128.8	137.5	186.4	160.9	113.7	85.06	86.82
$E'_{strain}{}^c$	134.5	172.7	121.5	126.6	136.4	122.0	111.6	77.18	51.13
$E''_{strain}{}^d$	126.9	163.6	113.8	118.8	129.6	112.7	107.9		

[a] Jahn−Teller axis modeled along N7−Cu−py3. [b] Jahn−Teller axis modeled along py1−Cu−py2 (see experimental structure). [C] single-point calculation of the optimized structure with all energies involving the metal ion set to zero (except for the $M-N-C_{backbone}$ potential), that is, strain imposed by the metal ion on the ligand. [d] $M-N-C_{backbone}$ term also excluded.

Table 3. Potentiometrically Determined Protonation and Complex Stability Constants (p*K* Values) of L^{6m} and L^{6o} [H_2O, $T = 25$ °C, $\mu =$ 0. 1 M (KCl)]

protonation constants	L^{6m}	L^{6o}
$L + H^+ \leftrightarrows [LH]^+$	**6.68**	**8.93**
$[LH]^+ + H^+ \leftrightarrows [LH_2]^{2+}$	**4.72**	**5.65**
$[LH_2]^{2+} + H^+ \leftrightarrows [LH_3]^{3+}$		**1.75**

stability constants with L^{6m}	Co^{2+}	Ni^{2+}	Cu^{2+}	Zn^{2+}	Li^+
$M^n + L \leftrightarrows [ML]^n$	**7.3**	**5.02**	**16.28**[a]	**9.18**	**3.7**
$[ML]^n \leftrightarrows [ML(OH)]^{n-1}$	8.9	8.6	9.07[b]	9.58	

stability constants L^{6o}	Co^{2+}	Ni^{2+}	Cu^{2+}	Zn^{2+}	Li^+
$M^n + [LH]^+ \leftrightarrows [MLH]^{n+1}$	5.78		10.93[b]		
$M^n + L \leftrightarrows [ML]^n$	**10.61**	**7.2**	**17.7**[a]	**12.52**	**3**
$[ML]^n \leftrightarrows [ML(OH)]^{n-1}$	10		10.4[b]	11.5	

[a] Formation of ML determined by ligand−ligand competition titrations in the ratio 1:1:1 ($M/L^{6m,o}/L'$); L′= EDTA, cyclam, PMIDA, or NTPH. [b] Determined by potentiometry and ligand−ligand competition.

these potentials are generally associated with small force constants and are assumed to be independent of the metal ion.[44,45] Nonbonded interactions (van der Waals terms) are also contributing; however, these are not decisive. A general observation that emerges from these hole-size curves for all bispidine-type ligands studied here (see Figure 3) is that, for large metal ions, there is practically no loss of ligand-based steric energy and, for averaged metal−donor distances smaller than approximately 2.0−2.1 Å, there is a buildup of ligand-based strain. This results from the fact that there is little constraint to fix the metal ion at a particular position in the ligand cavity, which is open on one side (see also the discussion on the elasticity of the coordination geometry above[21]). Smaller metal ions distort the ligand-based angles and distances, and this leads to a dramatic increase of the steric energy and a concomitant buildup of intraligand van der Waals repulsion. Note that these interpretations do not include the energetics of the metal−donor bonding (preference of the metal ion for specific donors, bond distances and coordination geometries, and electronic complementarity). The conclusion from the force field calculations is that, while the ligand L^{6m} is very rigid (as bispidine-type ligands are in general),[1,19] the coordination sphere is elastic and the ligand is not strongly size-selective, at least not for metal ions with average M−N bonds larger than approximately 2.1 Å, and has little preference for specific coordination geometries.[1] This interpretation from the force field calculations is in good agreement with the structural data (see above) and the stability constants (see below), but it is at variance with earlier predictions and molecular-mechanics-based interpretations with the derivative L^1.[11,12,46]

Solution Properties. The spectroscopic and electrochemical data of the cobalt(II), nickel(II), and copper(II) complexes of $L^{6m,e}$ and of some published compounds with mixed amine/pyridine donor sets are assembled in Table 4. The redox potentials and spectroscopic parameters are as expected; that is, because of the weak π donation/softness of the pyridine donors and the tolerance for long metal−donor bonds, lower oxidation states are stabilized (comparably high reduction potentials) and the ligand fields are relatively weak. A comparison of the spectroscopic properties of $[Cu(L^{6e})]^{2+}$ with those of the copper(II) complexes with L^{6m} and L^{3-5}

(44) Comba, P. *Coord. Chem. Rev.* **1993**, *123*, 1.
(45) Comba, P. *Coord. Chem. Rev.* **1999**, *182*, 343.

(46) A molecular-mechanics-based analysis of ML^1, using our approach and parametrization scheme,[1,19,32,43] indicates that the corresponding potential energy surface is also flat (see Figure 3 and Table 2). This is consistent with the similarity between L^1 and L^{3-6}, particularly with L^{6m}, and with our observed sets of stability constants (note that those for L^{3-5} are as expected, 2−6 orders of magnitude smaller, but follow similar general trends as those for $L^{6m,o}$, work in progress).

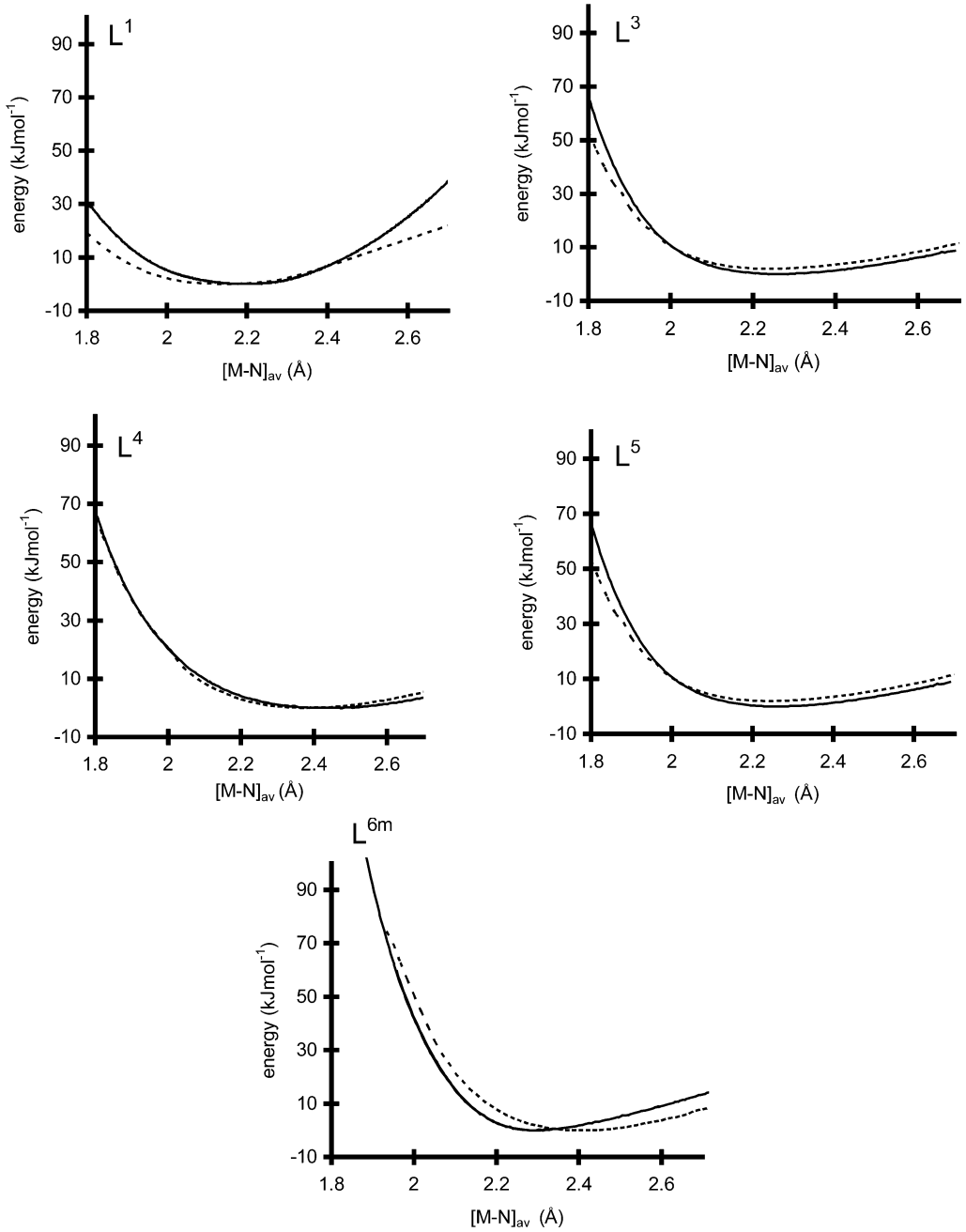

Figure 3. Hole-size curves of L^1, L^3, L^4, L^5, and L^{6m}. The energy minima of all curves were set to 0 kJ mol^{-1}. All curves are without metal-based potentials, except for C−N−M bending. Broken lines are with sum constraints; solid lines were obtained by individual, asymmetric variations of all six M−N bonds (linear interpolation and extrapolation between the longest and shortest observed distance for each M−N bond).

suggests that, in solution, the sixth donor (py3) might be coordinated.

Stability Constants. Polyamines and polyimines of a wide range of topologies have been the subject of detailed examinations of their stability constants with metal ions, and this work has been well-reported and reviewed.[2,47,48] The tetrakis-pyridine-substituted bispidine system $L^{6m,o}$ studied here is a ligand topology not yet examined and offers the capacity to encapsulate metal ions with six donors in a well-defined geometry. The structural and modeling studies reported above show that the ligands tolerate a rather wide variation in metal ion size without any significant strain. Despite the backbone rigidity, the coordination sphere is elastic and, thus, not predicted to be markedly size-selective (except for the destabilization of small metal ions); this can be probed by an examination of the thermodynamics of complexation with labile metal ions. The determined values of protonation and formation constants with selected metal ions for the $L^{6m,o}$ ligands appear in Table 3.

The ligand offers six protonation sites, but not all of the corresponding pK_a values could be determined because of the high acidity of some of the species (pK_a values: 6.68 and 4.72 for L^{6m} and 8.93, 5.65, and ∼1.75 for L^{6o}). The

(47) Smith, R. M.; Martell, A. E. *SSSA Spec. Publ.* **1995**, *42*, 7.
(48) Martell, A. E.; Smith, R. M. *Critical Stability Constants*; Plenum Press: New York, 1974−1989.

Table 4. Spectroscopic and Electrochemical Data of Co^{2+}, Ni^{2+}, and Cu^{2+} Complexes with Hexadentate Amine/Pyridine Ligands

	redox[a]		UV−vis (dd transition)[b]			EPR[c]			
	$3^+/2^+$	$2^+/1^+$	ν_1	ν_2	ν_3	$g_\parallel$	$g_\perp$	$A_\parallel$	ref
$[Co(L^{6m})]^{2+}$	+224		551/27 (sh)	493/67	397/170				
$[Co(L^{6e})]^{2+}$	+496		551/125 (sh)	504/166	371/323				
$[Co(L^3)(NO_3)]^+$	+372		536	509	466				39
$[Ni(L^{6m})]^{2+}$	irrev. $E_{pa} = +1387$	irrev. $E_{pa} = -1282$	815/30	532/18	304/443 (sh)				
$[Cu(L^{6m})]^{2+}$		−659	620/110			2.208	2.069	169	
$[Cu(L^{6e})]^{2+}$		−478	595/108			2.217	2.060	178	
$[Cu(L^3)(NCCH_3)]^{2+}$		−503	630/112			2.261	2.060	174	23
$[Cu(L^1)]^{2+}$			598						11,12
$[Cu(dap)]^{2+}$ [d]			604/143			2.215	2.053	196	71
$[Cu(ndap)]^{2+}$ [e]			604/110			2.216	2.056	196	72

[a] Redox potentials [mV] vs fc/fc^+. [b] λ_{max} [nm]/ϵ [M^{-1} cm^{-1}]. [c] $A_\parallel$ [10^{-4} cm^{-1}]. [d] dap = N,N-bis(2-pyridylmethylene-1,3-diaminopropane). [e] ndap = N,N-bis(2-pyridylmethylene-1,3-diamino-2-methyl-2-nitropropane).

first protonation occurs with a pK_a value close to 7 for L^{6m} and 9 for L^{6o}, which is surprisingly low if compared to the first pK_a of L^1.[11,12] This is associated with proton addition to a tertiary amine within the bispidine cavity. For L^1, this protonation most likely involves itself in bridging between the two rigidly disposed and adjacent nitrogen centers. For L^{6m}, these are very similar to those of tpen.[49,50] Because of lone pair repulsion in the free base, protonation or coordination to a metal ion should lead to a relief of steric strain, and this should enhance the stability of the protonated form as well as that of the metal complexes; this is particularly true for the macrocycle L^2, which, in the most stable structure, has the four N lone pairs directed to the centroid of the macrocycle.[1,17] A proton sponge effect was, therefore, observed in L^1 and L^2, which have a skeleton similar to that of L^{6m}; the pK_a values of L^1 and L^2 are 13.1[11,12] and approximately 24,[51] respectively. Part of the reason for this difference might be that there are changes in the nucleophilicity of the nitrogen donors of the tertiary amines between L^1, L^2, and L^6, due to substituents at the ligand backbone in L^6 (two ester, one ketone, and two additional methylpyridine groups). A chair-boat equilibrium in the protonated free ligand also cannot be excluded (see above), although the structure of the free ligand (see Figure 1) does not seem to support this interpretation.

As a result of substituent effects, the two tertiary amines gain electron density by the aliphatic substituents and suffer from a withdrawal of electron density by the picolyl groups, which are, according to an empirical method for the prediction of protonation constants, responsible for a decrease of approximately 2 log units.[49] In the case of L^{6m}, the two additional picolyl groups as well as the keto and two ester substituents further reduce the nucleophilicity of the amine donors. This results in a decrease of the "cavity effect", yielding pK_a values for the amine donors close to those of tpen (pK_a 7.38, 4.84, 3.24, and 2.82).[49] The successive protonation of the pendant pyridine groups becomes progressively more difficult as the charge on the ligand rises to a level where protonation is barely accessible in dilute aqueous acidic solutions of low ionic strength (0.1 M). The ligand L^{6m} undergoes an irreversible reaction with the base at pHs larger than 10, which is avoided in the fully reduced ligand L^{6o}. The decrease of pK_a by the OH substituents is smaller than that of the carbonyl groups, and therefore, the observed protonation constants of the fully reduced ligand L^{6o} are larger.

Metal−ligand complexation systems with rigid (macrocyclic) ligands have been modeled, in general, with a common and relatively simple model, featuring the formation of ML, MLH, and MLH_{-1} species,[52] and likewise, this can be applied here. However, the computed appearance of MLH could also be an artifact, due to a kinetic effect in the formation of the ML complex.

An additional deprotonation equilibrium can be observed in all complexes, except in those of Li^+ with $L^{6m,o}$ and Ni^{2+} with L^{6o}, after the equivalents of acid originally present in solution are consumed. For L^{6m}, the corresponding log K values are very similar, that is, approximately 9.0. Since the deprotonation of a water molecule coordinated to a metal center might involve the elimination of a pyridine donor in a basic medium, to exchange with water, and since the values for the hydrolysis would be expected to be quite varied for the different metal ions (independently of a six- or seven-coordinate geometry), a quite constant value of 9.0 is unexpected. For all crystal structures of the complexes with L^{6m}, the hydrated form of the 9-keto group was found. The observed deprotonation might, therefore, be at this position, and this might eventually lead to ligand decomposition. The somewhat larger variation in the L^{6o} systems suggests that seven-coordination and deprotonation of the coordinated OH_2 might be an alternative for this ligand. This is in agreement with the observation of seven-coordinate bispidine complexes[19,26] and the corresponding electronic spectra.

Only 1:1 complexation was modeled throughout; no evidence for M_2L species was forthcoming nor has any been provided to any substantial degree by any other spectroscopic or structural technique. These ligands, which offer six potential donor groups in a rigid arrangement for binding metal ions and present a coordination environment sufficiently elastic to accommodate many different metal ions, determinedly form 1:1 species. Consequently, for compara-

(49) Cukrowski, I.; Cukrowska, E.; Hancock, R. D.; Anderegg, G. *Anal. Chim. Acta* **1995**, *312*, 307.
(50) Anderegg, G.; Hubmann, E.; Podder, N. G.; Wenk, F. *Helv. Chim. Acta* **1977**, *60*, 123.
(51) Comba, P.; Kerscher, M.; Kleditzsch, L.; Oeser, T.; Schiek, W. Manuscript in preparation.
(52) Wei, G.; Hambley, T. W.; Lawrance, G. A.; Maeder, M. *Aust. J. Chem.* **2002**, *55*, 667.

tive purposes, it was the value of K_{ML} that we particularly sought. The efficient encapsulation of metal ions by the hexadentate ligand L^{6m} is also supported by the fact that, in general, no metal ion exchange was observed in neutral aqueous solutions within several weeks.

Since, for Cu^{2+}, complexation reactions were found to be complete over the entire accessible pH range (2−11), ligand−ligand competition titrations were also performed in the ratio 1:1:1 ($M/L^{6m,o}/L'$). Various competing ligands L′ were explored in order to be able to observe partial formation of the $ML^{6m,o}$ complexes. Also, pH titrations were simultaneously followed with UV−vis spectroscopy, which provided help in identifying the formation of the various species. These absorbance data were fitted simultaneously with Hyperquad, and the resulting spectra of the ML species were, where applicable, in acceptable agreement with those measured separately (see Table 4). This is taken as additional evidence for the correctness of the model used for the fitting of the stability constants.

Because of the slower kinetics of Ni^{2+} complex formation, these titrations were performed with long delay times after base addition. For L^{6m} in very basic media (pH > 10), this led to the decomposition of small amounts of the metal-free ligand present in solution, and this also slowly led to complex degradation. This is observed by the appearance of an intense transition near 450 nm, which also appears in the titration of the metal-free ligand. This effect obviously limits the accuracy of the data, at least at high pH. However, the ML species are defined in a pH region where the system is better behaved.

For the d^0 and d^{10} metal ions studied here (Zn^{2+} and Li^+), ligand field effects are absent and size selectivity is more important than it is for the open-shell systems. The fact that the stabilities for Zn^{2+} and Li^+, with similar $\sum_{i=1}^{6}(M - N_i)$ values (see Table 1) and similar ionic radii (Li^+ 0.76 Å and Zn^{2+} 0.74 Å), are very different suggests that the metal ion size and steric strain are not the only factors of importance. The ionic radii (Co^{2+} 0.75 Å, Ni^{2+} 0.69 Å, Cu^{2+} 0.75 Å, and Zn^{2+} 0.74 Å) and the observed (Table 1) and computed (Table 2) bond distances [$\sum_{i=1}^{6}(M - N_i)$, Co^{2+} 12.8 Å, Ni^{2+} 12.6 Å, Cu^{2+} ∼13 Å, and Zn^{2+} 13.1 Å] suggest that size-match selectivity is of some importance, but with the relatively flat potential energy surfaces (see above and Figure 3) and the large differences in stability constants, this probably is not a major effect. An inspection of the averaged M−N distances suggests that, for Co^{2+} and Ni^{2+}, these are smaller (∼2.1 Å, see Tables 1 and 2) than optimal in terms of the ligand preference (∼2.2−2.3 Å, see Figure 3) and, therefore, are elongated by the ligand; that is, there is some strain induced to the metal−donor bonds. As a result of the Jahn−Teller lability and the ligand geometry which ideally accounts for this,[18,19,21,27,28,31] the Cu^{2+}/L^{6m} system is highly complementary. The larger Zn^{2+} center with relatively weak M−N force constants and virtually no angular directionality also ideally fits the ligand requirements. A semiquantitative interpretation emerges from the computed strain energies [Table 2; E'_{strain} (strain induced to the ligand by metal ion coordination)]. Coordination to very small metal ions (Co^{3+} and Cr^{3+}) leads to large distortions (loss of up to 60 kJ/mol with respect to the relatively unstrained geometry induced by Zn^{2+}; see also the relatively high redox potential of the $Co^{3+/2+}$ couple above); coordination to Co^{2+} and Ni^{2+} still leads to a loss in steric energy of more than 10 kJ/mol relative to Zn^{2+} (as a result of the Jahn−Teller-induced tetragonal geometry and the electronic stabilization, Cu^{2+} is excluded from this discussion).

On the basis of simple thermodynamics, the energy difference of approximately 10 kJ/mol can be translated to a difference of approximately 2 log units in the stability constants; that is, part of the relatively high stability of the zinc(II) complex is due to a good fit. The relatively low stability of Ni^{2+} might be due to the generally larger preference of Ni^{2+} for angular directionality (larger in-plane ligand field; highly distorted geometry in the bispidine complexes), and this is not included in the force field calculations.

Experimental Section

Measurements and Materials. Chemicals for the syntheses and solvents were of the highest degree of purity and were used without further purification. The piperidine precursor pL^{6m} and the corresponding ligand L^{6m} were prepared as described before.[24]

UV−vis−NIR spectra were recorded in CH_3CN at room temperature on a Cary 1 or Cary 2500 spectrophotometer. IR spectra were obtained from KBr pellets, measured with a Perkin-Elmer 16C FT-IR instrument. NMR spectra were recorded at room temperature on a Bruker AS 200 (200.13 MHz for ^1H) spectrometer; the chemical shifts (δ, ppm) are relative to TMS or the solvent as an internal standard.

Electrochemical measurements [cyclic voltammetry (100 mV/s), 2×10^{-3} M complex solutions] were done on a BAS100B system (data analysis with Digisim) with a glassy carbon working electrode, a Pt-wire auxiliary, and a $Ag/AgNO_3$ reference electrode (0.01 M $AgNO_3$);[53] 0.1 M tetrabutylammoniumhexafluorophosphate in acetonitrile was used as the electrolyte and, ferrocene was used as an external standard. EPR spectra were recorded with a Bruker ELEXSYS E500 spectrometer (approximately 10^{-3} M frozen solutions in 2:1 DMF/H_2O) at 130 K. Xsophe, version 1.1.4, operating on a LINUX workstation was used for the computer simulation of the spectra.[54,55]

Potentiometric titrations were performed on 20 cm^3 samples at the metal ion concentration of 1.0×10^{-3} mol dm^{-3} with a metal-to-ligand ratio of 1:1. The measurements were made with a pH meter equipped with a 6.0202.100 combined electrode (Metrohm) and a 665 Dosimat automatic buret (Metrohm), containing a carbonate-free stock solution of tetrabuthylamonium hydroxide ∼0.1 M, standardized by titrating potassium hydrogen phthalate. For each measurement, 120−240 titration points were recorded. During the titration, a slight nitrogen stream was passed over the sample solution to ensure the absence of carbon dioxide. All pH measurements were carried out at a constant ionic strength (μ = 0.1 mol dm^{-3} KCl) and constant temperature (T = 298 K) (pKw = 13.78). The overall stability constants were calculated with Hyperquad, with pH as well as with absorbance data recorded simultaneously by a TIDAS II (J&M) spectrophotometer, equipped with an external

(53) Noviandri, I.; Brown, K. N.; Fleming, D. S.; Gulyas, P. T.; Lay, P. A.; Masters, A. F.; Phillips, L. *J. Phys. Chem.* **1999**, *103*, 6713.
(54) Wang, D.; Hanson, G. R. *Appl. Magn. Reson.* **1996**, *11*, 401.
(55) Wang, D.; Hanson, G. R. *J. Magn. Reson. A* **1995**, *117*, 1.

immersion probe 661.202UVS from Hellma. The proton equilibrium was confirmed by Bjerrum charts.[56] For each system, each titration was repeated at least three times, with good reproducibility (~ ±0.01 pH units). The instability of the ligand L^{6m} at high pH as well as the stability of its triol were shown by back-titrations with 0.1 M HCl and a second titration with Bu_4NOH to the reacidified sample. This instability in basic media of L^{6m} was also observed in mixtures of 70:30 and 50:50 H_2O/dioxane and in pure methanol. The solubility of L^{6m} is low, and therefore, the determination of its pK_a values was done in samples at a concentration of 0.5 mM. Although, at low pH, retro-Mannich reactions might be a problem, this was not observed. The difference between equivalence points in the titration of the free ligand is as expected for the weighed quantity (see the Supporting Information). For the determination of the formation constants with Cu^{2+}, which, during the entire titration, is fully complexed, 1:1:1 ligand−ligand competition titrations were performed. Various competing ligands with known pK_a values and complex formation constants {EDTA (1,2-diaminoethane-N,N,N′,N′-tetraethanoic acid),[57−59] cyclam(1,4,8,11-tetraazacyclotetradecane),[60−62] NTPH [nitrilotris(methylphosphonic acid)],[63,64] and PMIDA (N-phosphonomethyl)iminodiethanoic acid[65]} were used to confirm the titration results.

Mass spectra were recorded on a Finnigan 8400 spectrometer (EI or FAB), with a nitrobenzyl alcohol matrix (Nibeol, NBA) for the FAB spectra.

Elemental analyses were obtained from the microanalytical laboratory of the University of Heidelberg.

Ligand Syntheses. The piperidine precursor pL^{6e} [dimethyl-4-oxo-2,6-di-(2-pyridyl)-1-(2-pyridylethyl)-piperidin-3,5-dicaboxylate] was obtained by a dropwise addition of pyridine-2-aldehyde (9.56 cm^3, 100 mmol) and 2-aminoethylpyridine (5.4 cm^3, 44 mmol) to an ice-cold solution of dimethyl acetonedicarboxylate (6.4 cm^3, 44 mmol) in MeOH (30 cm^3). After 5 min, the orange solution was stored in a freezer (−18 °C), and the crystallized product was collected after several days, washed with cold EtOH, and recrystallized from EtOH; a further crop could be obtained by evaporation of the filtrate. Yield: 16.58 g, 35 mmol, 80%.

$L^{6m/e}$. To a solution of $pL^{6m/e}$ (15.0 g, 32.6 mmol/16.0 g, 33.8 mmol) in 25 cm^3 THF was added 2-(aminomethyl)pyridine/2-(aminoethyl)pyridine (4.0 cm^3, 39.1 mmol/4.85 cm^3, 40.5 mmol) and a 37% aqueous formaldehyde solution (6.4 cm^3, 78.3 mmol/7.3 cm^3, 81.0 mmol). The mixture was stirred under reflux for 4 h; a deep black solution resulted. The solvent was removed under low pressure, and the remaining dark brown solid was recrystallized from ethanol. Yield for L^{6m}/L^{6e} (white solid): 4.75 g, 8.02 mmol, 25%/11.23 g, 18.1 mmol, 54%. Anal. Calcd for $C_{35}H_{32}N_6O_5 \cdot 2H_2O$: C, 63.09; H, 5.77; N, 13.37%. Found: C, 63.27; H, 5.90; N, 13.77%. Anal. Calcd for $C_{36}H_{36}N_6O_5$: C, 67.73; H, 5.85; N, 13.54%. Found: C, 67.46; H, 5.93; N, 13.43%. FAB^+ MS (Nibeol): 594 (M^+), 621(M^{-1}). ^1H NMR (300.133 MHz, $CDCl_3$): 2.87 (d, 2H, $^2J_{HH}$ = 12.0 Hz, N−C***H***$_2$), 3.45 (d, 2H, $^2J_{HH}$ = 12.0 Hz, N−C***H***$_2$), 3.65 (s, 6H, OC***H***$_3$), 3.67 (s, 4H, N−C***H***$_2$−Py), 5.28 (s, 2H, N−C***H***), 6.78 (d, 2H, $^3J_{HH}$ = 7.7 Hz, Ar-***H***), 7.02−7.20 (m, 2H, Ar-***H***), 7.39 (td, 2H, $^3J_{HH}$ = 7.7 Hz, $^4J_{HH}$ = 1.8 Hz, Ar-***H***), 7.46 (td, 2H, $^3J_{HH}$ = 7.7 Hz, $^4J_{HH}$ = 1.8 Hz, Ar-***H***), 7.84 (d, 2H, $^3J_{HH}$ = 7.7 Hz, Ar-***H***), 8.44 (m, 4H, Ar-***H***), 8.61 (d, 2H, $^3J_{HH}$ = 4.0 Hz, Ar-***H***).

L^{6o}. Sodium tetrahydroborate (1.92 g, 0.0507 mol) was added slowly to a cooled suspension of L^{6m} (3.0 g, 5.06 mmol) in 75 mL of absolute MeOH; the temperature remained below 0 °C. After the solution had stirred at room temperature for 20 h, the solvent was removed under reduced pressure. The solid product was dissolved in water (120 mL), and the solution was stirred for 2 h. The white suspension was extracted with $CHCl_3$ (120 mL), the solvent removed, and the solid stirred in hydrochloric acid (10%, 60 mL) for 1 h. After neutralization with NaOH and extraction with $CHCl_3$ (120 mL), the organic phase was dried over magnesium sulfate; the removal of the solvent under reduced pressure produced a white solid (2.88 g, crude). To a solution of this product in absolute THF (60 mL) was added dropwise a filtered solution of $LiAlH_4$ (1 M in THF, 19.6 mL). After stirring for 20 h at room temperature, the yellow paste was treated with an aqueous solution of sodium tartrate (4.5 g, 19.6 mmol). The two layers were separated and the aqueous phase extracted three times with chloroform (100 mL). The organic phases were collected, and the same volume of chloroform was added. The water phase was removed, and the organic phase was dried over $MgSO_4$. The removal of the solvent under reduced pressure yielded 1.4 g of a yellow foam. Recrystallization from THF/Et_2O yielded a fine white powder: 0.8 g (1.5 mmol, 30%). Anal. Calcd for $C_{31}H_{34}N_6O_3 \cdot {}^1/_2THF$: C, 68.85; H, 6.83; N, 14.60%. Found: C, 68.04; H, 6.69; N, 14,37%. mp 160 °C (dec). ^1H NMR (200.133 MHz, $CDCl_3$): 1.77 (dd, 4H, $^2J_{HH}$ = 10.6 Hz, N−C***H***$_2$), 2.40 (d, 2H, $^2J_{HH}$ = 12.4 Hz, N−C***H***$_2$), 3.33 (s, 2H, N−C***H***$_2$−Py), 3.606 (s, 2H, N−C***H***$_2$−Py), 3.68−3.76 (m, 4H, C***H***$_2$−OH, $^4J_{HH}$ = 4−4.2 Hz, different signals due to internal H bonds with pyridine groups), 3.8 [s, 1H, C**H**(OH)], 5.08 (s, 2H, N−C***H***), 6.72−8.52 (m, 16H pyridine, diverse group of signals due to variable internal H bonds with OH groups). IR: The disappearance of the signals at 1720, 1350, 1270, and 1200 cm^{-1}, present in L^{6m} and associated with carbonyl and ester groups, was observed, whereas the vibrations of the pyridine rings were intact (four intense bands from 1400 to 1600 cm^{-1}).

Complex Syntheses, General Method. To a solution of 1 mmol of the ligand ($L^{6m/e/o}$) in acetonitrile (1 cm^3) was added a solution of 1 mmol of the metal salt in methanol (1 cm^3). The mixture was stirred for 24 h, the solvent was then evaporated, and the resulting solid was washed two times with EtOAc and dried in vacuo. The pure products were isolated in 40−70% yield, and crystals were obtained by ether diffusion to solutions of the pure complexes in acetonitrile. Full details of the characterization of the complexes are given in the Supporting Information.

Crystal Structure Determination. Crystal data and details of the structure determinations are listed in Table 5. Intensity data were collected for **a** on a Syntex R3; for **c** and **e** on a Siemens-Stoe AED2 diffractometer; and for **b**, **d**, **f**, and **g** on a Bruker AXS SMART 1000 CCD area detector (Mo Kα radiation, λ = 0.710 73 Å, ω-scan; see Table 5 for definitions of **a**−**g**). The structures were solved by direct methods and refined by full matrix least-squares, based on F^2, with all reflections using the SHELXTL programs.[66]

Hydrogen atoms were inserted in calculated positions (**a**, **d**, **f**, and **g**) or located in difference Fourier maps (**b**, **c**, and **e**). For **f** and **g**, corrections for disordered solvent molecules and anions were applied using the SQUEEZE routine of the program system PLATON.[67]

(56) Avdjeef, A. *Curr. Top. Med. Chem.* **2001**, *1*, 277.
(57) Delgado, R.; Quintino, S.; Teixeira, M. *J. Chem. Soc., Dalton Trans.* **1997**, 55.
(58) Anderegg, G. *IUPAC Chem. Data Ser.* **1978**, *14*.
(59) Baumann, E. *J. Inorg. Nucl. Chem.* **1974**, *36*, 1827.
(60) Hancock, R.; Motekaitis, R.; Cukrowski, I. *J. Chem. Soc., Perkin Trans. 2* **1996**, 1925.
(61) Motekaitis, R.; Rogers, B.; Reichert, D. *Inorg. Chem.* **1996**, *35*, 3821.
(62) Buffle, J.; Staub, C. *Anal. Chem.* **1984**, *56*, 2837.
(63) Sawada, K.; Miyagawa, K.; Sakaguchi, T. *J. Chem. Soc., Dalton Trans.* **1993**, 3777.
(64) Sawada, K.; Araki, T.; Suzuki, T. *Inorg. Chem.* **1989**, *28*, 2687.
(65) Dhansay, M.; Linder, P. *J. Coord. Chem.* **1993**, *28*, 2687.

Table 5. Crystallographic Data

	L^{6m} (**a**)	$[Li(L^{6o})]ClO_4 \cdot 0.5CH_3OH$ (**b**)	$[Ni(L^{6m})](ClO_4)_2 \cdot 3H_2O$ (**c**)	$[Cu(L^{6m})](ClO_4)_2 \cdot 2H_2O$ (**d**)
empirical formula	$C_{33}H_{32}N_6O_5$	$C_{31.5}H_{39}ClLiN_6O_7$	$C_{33}H_{38}Cl_2N_6NiO_{16}$	$C_{33}H_{36}Cl_2CuN_6O_{15}$
fw	592.65	664.08	904.30	891.12
temp	298(2)	173(2)	203(2)	173(2)
cryst syst	monoclinic	monoclinic	monoclinic	orthorhombic
space group	$P2_1/c$	$P2_1/n$	$P2_1/c$	$Pca2_1$
unit cell dimensions [Å, deg]	$a = 11.347(2)$	$a = 8.3466(6)$	$a = 10.526(5)$	$a = 35.955(2)$
	$b = 14.543(3)$	$b = 20.5064(14)$	$b = 18.473(9)$	$b = 10.4683(6)$
	$c = 18.596(3)$	$c = 18.4362(13)$	$c = 19.567(10)$	$c = 19.1971(10)$
	$\beta = 104.95(1)$	$\beta = 93.259(1)$	$\beta = 102.29(4)$	$\beta = 90$
vol [Å^3]; Z	2964.8(9); 4	3150.4(4); 4	3718(3); 4	7225.6(7); 8
density (calcd) [g cm^{-3}]	1.328	1.400	1.616	1.638
abs coeff [mm^{-1}]	0.092	0.181	0.750	0.835
F(000)	1248	1400	1872	3672
cryst size [mm]	0.60 × 0.50 × 0.40	0.25 × 0.22 × 0.07	0.75 × 0.20 × 0.20	0.42 × 0.34 × 0.30
θ max	24.00	24.71	25.00	28.30
reflns collected	4870	16934	6549	48 910
independent reflns	4648 [0.0345]	5352 [0.0429]	6549	17 038 [0.036]
params	403	576	675	1105
final R1 [$I > 2\sigma(I)$]	0.0701	0.0566	0.0460	0.0480
wR2 (all data)	0.1688	0.1697	0.1096	0.1247
largest diff. peak/hole [e Å^{-3}]	0.201/−0.27	0.70/−0.44	0.32/−0.38	1.50/−0.59

	$[Zn(L^{6m})](ClO_4)_2 \cdot 3H_2O$ (**e**)	$[Co(L^{6e})](PF_6)_2 \cdot H_2O$ (**f**)	$[Cu(L^{6e})](ClO_4)_2 \cdot H_2O$ (**g**)
empirical formula	$C_{33}H_{38}Cl_2N_6O_{16}Zn$	$C_{35}H_{38}CoF_{12}N_6O_6P_2$	$C_{41.5}H_{50}Cl_2CuN_6O_{14}$
fw	910.96	987.58	991.32
temp	203(2)	173(2)	173(2)
cryst syst	monoclinic	orthorhombic	monoclinic
space group	$P2_1/c$	$P2_12_12_1$	$P2_1/c$
unit cell dimensions [Å, deg]	$a = 10.535(5)$	$a = 13.8725(7)$	$a = 10.6086(1)$
	$b = 18.449(9)$	$b = 25.2296(14)$	$b = 23.8635(4)$
	$c = 19.650(10)$	$c = 25.3959(13)$	$c = 17.1253(3)$
	$\beta = 102.20(4)$	$\beta = 90$	$\beta = 105.788(1)$
vol [Å^3]; Z	3733(3); 4	8888.5(8); 8	4171.9(1); 4
density (calcd) [g cm^{-3}]	1.621	1.476	1.578
abs coeff [mm^{-1}]	0.885	0.557	0.730
F(000)	1880	4024	2064
cryst size [mm]	0.60 × 0.55 × 0.35	0.27 × 0.20 × 0.18	0.40 × 0.17 × 0.11
θ max	27.00	21.97	27.11
reflns collected	8150	37 643	36 179
independent reflns	8150	10 890 [0.066]	9187 [0.048]
params	675	869	495
final R1 [$I > 2\sigma(I)$]	0.0423	0.0496	0.0502
wR2 (all data)	0.1080	0.1059	0.1394
largest diff. peak/hole [e Å^{-3}]	0.48/−0.45	0.26/−0.21	1.04/−0.58

Molecular Modeling. For the empirical force field calculations, the MOMEC program[68] and force field[69] were used. Parameters for the Jahn−Teller labile Cu(II)−bispidine complexes were taken from the literature.[1,19] The technique to compute metal-ion-independent hole-size curves has been described,[32] discussed, and validated.[1,70]

Acknowledgment. Generous financial support by the Deutsche Forschungsgemeinschaft (DFG), the provision of facilities by the University of Heidelberg, and support by the University of Newcastle for G.A.L. to undertake an outside studies program are gratefully acknowledged.

Supporting Information Available: Comparative titration curves for the ligands L^{6m} and L^{6o} as well as species distribution curves for the free ligands and systems containing metal ions and the ligands in 1:1 molar ratios. Full details of the characterization of the metal complexes. This material is available free of charge via the Internet at http://pubs.acs.org.

IC0513383

(66) Sheldrick, G. M. *SHELXTL NT*, version 5.10; Bruker AXS: Madison, WI, 1999.
(67) Spek, A. *PLATON*; Universität Utrecht: Utrecht, The Netherlands, 1990.
(68) Comba, P.; Hambley, T. W.; Lauer, G.; Melter, M.; Okon, N. *MOMEC97, a molecular modeling package for inorganic compounds*; University of Heidelberg: Heidelberg, Germany, 1997. www.comba-group.uni-hd.de.
(69) Bol, J. E.; Buning, C.; Comba, P.; Reedijk, J.; Ströhle, M. *J. Comput. Chem.* **1998**, *19*, 512.
(70) Comba, P.; Hambley, T. W. *Molecular Modeling of Inorganic Compounds*, 2nd ed.; Wiley-VCH: Weinheim, Germany, 2001. Includes a tutorial based on MOMEClite, 2nd ed.
(71) Nikles, D. E.; Powers, M. J.; Urbach, F. L. *Inorg. Chem.* **1983**, *22*, 3210.
(72) Comba, P.; Hambley, T. W.; Lawrance, G. A. *Helv. Chim. Acta* **1985**, *68*, 2332.